FISEVIER

Contents lists available at ScienceDirect

Nuclear Inst. and Methods in Physics Research, B

journal homepage: www.elsevier.com/locate/nimb





In-source and in-trap formation of molecular ions in the actinide mass range at CERN-ISOLDE

M. Au a,b,*, M. Athanasakis-Kaklamanakis a,c, L. Nies a,d, J. Ballof a,e, R. Berger a,f, K. Chrysalidis a, P. Fischer d, R. Heinke a, J. Johnson c, U. Köster a,g, D. Leimbach a,1, B. Marsh a, M. Mougeot a,h,2, B. Reich a, J. Reilly i, E. Reis a, M. Schlaich j, Ch. Schweiger a,h, L. Schweikhard d, S. Stegemann a, J. Wessolek a,i, F. Wienholtz j, S.G. Wilkins a,k, W. Wojtaczka c, Ch.E. Düllmann b,l,m, S. Rothe a

- ^a CERN, Geneva, Switzerland
- ^b Johannes Gutenberg-Universität Mainz, Mainz, Germany
- c KU Leuven, Leuven, Belgium
- ^d Universität Greifswald, Greifswald, Germany
- e FRIB, Michigan State University, East Lansing, MI, United States of America
- f Philipps-Universität Marburg, Marburg, Germany
- g Institut Laue-Langevin, Grenoble, France
- ^h Max Planck Institut für Kernphysik, Heidelberg, Germany
- ¹ The University of Manchester, Manchester, United Kingdom
- ^j Technische Universität Darmstadt, Darmstadt, Germany
- ^k Massachusetts Institute of Technology, Cambridge, United States of America
- ¹ GSI Helmholtzzentrum für Schwerionenforschung, Darmstadt, Germany
- ^m Helmholtz Institute Mainz, Mainz, Germany

ARTICLE INFO

Keywords: Radioactive molecules Molecular ion beams Isotope Separation On Line Actinides Mass spectrometry

ABSTRACT

The use of radioactive molecules for fundamental physics research is a developing interdisciplinary field limited dominantly by their scarce availability. In this work, radioactive molecular ion beams containing actinide nuclei extracted from uranium carbide targets are produced via the Isotope Separation On-Line technique at the CERN-ISOLDE facility. Two methods of molecular beam production are studied: extraction of molecular ion beams from the ion source, and formation of molecular ions from the mass-separated ion beam in a gas-filled radio-frequency quadrupole ion trap. Ion currents of U^+ , UO_{1-3}^+ , UC_{1-3}^+ , UF_{1-4}^- , $UF_{1,2}O_{1,2}^+$ are reported. Metastable tantalum and uranium fluoride molecular ions are identified. Formation of UO_{1-3}^+ , $U(OH)_{1-3}^+$, UC_{1-3}^+ , $UF_{1,2}O_{1,2}^+$ from mass-separated beams of U^+ , $UF_{1,2}^+$ with residual gas is observed in the ion trap. The effect of trapping time on molecular formation is presented.

1. Introduction

There is interdisciplinary interest in radioactive molecules bridging fields of molecular physics, atomic physics and nuclear physics, as well as physics beyond the standard model [1]. Experimental research possibilities with many radioactive molecules are currently constrained by their limited production. This is particularly the case for radioactive molecules containing an actinide element. Only actinides in the decay chains of primordial $^{232}{\rm Th}$ and $^{235,238}{\rm U}$ are available in macroscopic quantities in nature. All others must be produced artificially.

The Isotope Separation On-Line (ISOL) method allows production of a wide range of radioactive nuclides across the nuclear chart through reactions induced by the impact of an accelerated particle beam hitting a thick target. The ISOLDE facility at CERN [2] uses 1.4-GeV protons accelerated by CERN's Proton Synchrotron Booster (PSB) and can employ a variety of target and ion source systems. Once created, the reaction products must diffuse out of the target material and effuse to the ion source, where they are ionized and extracted as a beam of charged particles. For refractory species, forming volatile compounds has been employed as a technique to improve extraction from the target

^{*} Corresponding author at: CERN, Geneva, Switzerland. E-mail address: mia.au@cern.ch (M. Au).

¹ Present address: University of Gothenburg, Sweden.

² Present address: University of Jyväskylä, Finland.

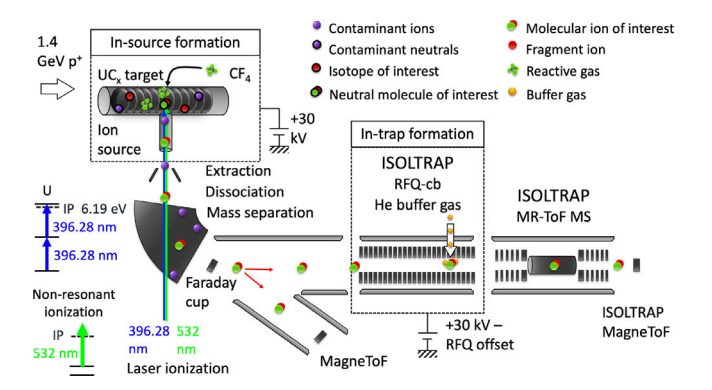


Fig. 1. Schematic of the experimental setup. Molecules are generated in the UC_x target or from the mass-separated ion beam in the ISOLTRAP RFQ-cb. The mass-separated beam is sent to a MagneToF detector or bunched and sent to the MR-ToF MS for identification. The uranium resonant ionization scheme shown uses a single titanium:sapphire laser [14].

by delivering the isotopes of interest as molecular ion beams [3–6]. In specific cases, the formation of molecules can reduce the isobaric contamination remaining after mass separation. The production of actinide molecules could address the scarcity and purity problems limiting many experiments on actinide isotopes. In addition, they present promising cases themselves [1.7–9].

2. Method

The ISOLDE facility was used to study actinide species produced from four porous micro-structured uranium carbide (UC_x) target units: a previously-irradiated target coupled to a rhenium surface ion source; a previously-irradiated target coupled to a tungsten surface ion source; and two new targets coupled to Forced Electron Beam Induced Arc Discharge (FEBIAD) ion sources [10]. The ISOLDE Resonance Ionization Laser Ion Source (RILIS [11]) was used to resonantly ionize atomic U with the ionization scheme shown in Fig. 1. Ion beams were extracted from the ion source using a 30-kV potential difference and separated by their mass-to-charge ratio in the separator magnet. Mass-separated ion beams were either sent to a MagneToF detector or cooled and bunched in the ISOLTRAP Radio-Frequency Quadrupole cooler-buncher (RFQ-cb) [12]. The bunched beam was sent to the Multi-Reflection Time-of-Flight Mass Spectrometer (MR-ToF MS) [13], where ions were separated based on their mass-to-charge ratios, including isobars, which were identified through ToF mass measurements. The experimental setup is shown schematically in Fig. 1.

3. In-source molecular formation

The target units with the tungsten surface ion source and the two FEBIAD type ion sources were equipped with calibrated leaks $(1.3\times10^{-4},\,3\times10^{-4}\,$ and $5.7\times10^{-5}\,$ mbar L s $^{-1})$ through which carbon tetrafluoride (carbon tetrafluoromethane, CF $_4$) gas was injected as a reagent for fluoride molecule formation. Using the two different types of ion sources, surface-, electron-impact-, and non-resonantly laser-ionized-molecules were observed. Nominal operating temperatures for a UC atraget and the different ion sources are near 2000 °C. Some measurements were performed with different experimental parameters where indicated such as in the captions of Figs. 2 and 3.

Uranium molecules from the target material and tantalum molecules from the target container were identified using mass scans performed with the ISOLDE mass separator magnets (Fig. 2) and verified using the ISOLTRAP MR-ToF MS. $^{235,238}\text{U}$ are present in the target as well as trace amounts of ^{234}U as a product of ^{238}U decay. These formed UO+ and UO+ with $^{16,18}\text{O}$ present from residual gas or oxide residues in the target. Depending on the degree of oxidation, the molecular oxide

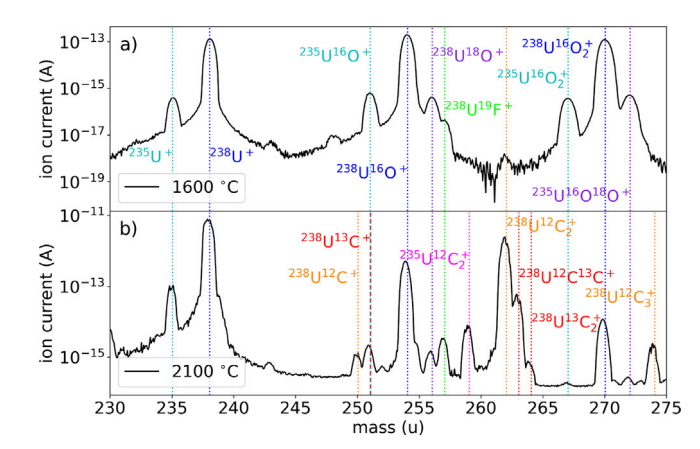


Fig. 2. Ion beam current recorded on the MagneToF detector during a scan of the GPS mass separator magnet showing the surface-ionized molecules from a rhenium ion source coupled to a previously irradiated $\rm UC_x$ target at a target temperature of (a) 1600 °C and (b) 2100 °C. Note the logarithmic scale.

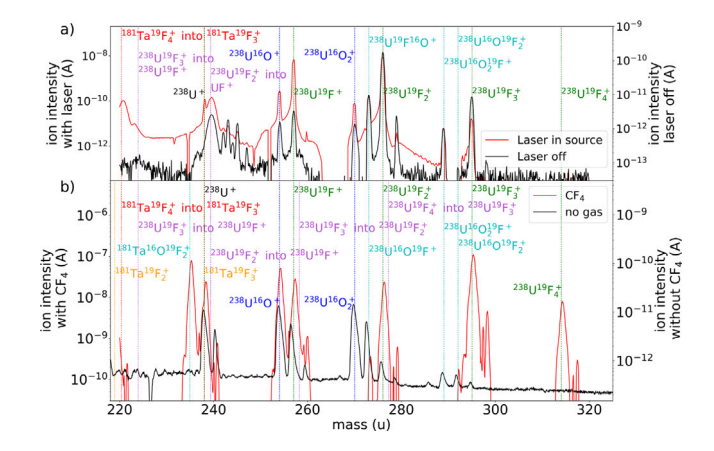


Fig. 3. Mass spectra of ion beams from UC_x targets using the GPS mass separator magnet. (a) a tungsten surface ion source with CF_4 gas injection through a calibrated leak for an ion source internal pressure of approximately 1.6×10^{-4} mbar without (black) and with 38 W of 532-nm laser light at a repetition rate of 10 kHz (red). Target at 1650 °C and ion source at 1370 °C. (b) a FEBIAD ion source before (black) and after injection of CF_4 through a calibrated leak for an ion source internal pressure of approximately 7.5×10^{-5} mbar (red). Target at 1200 °C and ion source at 1830 °C.

ion intensity decreased with time and target heating in the presence of excess carbon from the UC_x target. At higher temperatures, uranium carbides (UC+ and UC_2+) were observed, formed from both $^{12,13}\mathrm{C}$ (Fig. 2). With the addition of CF_4, UF_1,2,3 and UFO+ dominated the total surface- or plasma-ionized beam. Details of experimental parameters are given in Fig. 3.

3.1. Non-resonant laser and plasma ionization

UO+ and UO₂+ dominate the ion beam for oxidized targets. With first ionization potentials of 6.0313(6) eV and 6.128(3) eV for UO and UO₂, respectively [15], these species are observed with both surface and FEBIAD ion sources. With CF₄ injection, tungsten surface ionization, and 30 W of 532-nm laser light, UF+ and UF₂+ are the most intense uranium molecular ion beams. Surface-ionized UF₃+ is detectable with a Faraday Cup; UF₄+ is not observed (Fig. 3 (a)). Using a FEBIAD ion source, the UF₃+ sideband is dominant and UF₄+ is observed. Higher rates of U+ likely result from the breakup of uranium molecules in the FEBIAD ion source before extraction as an ion beam. Sideband ratios depend strongly on the concentration of CF₄, favoring UF_{2,3}+ with higher leak rates of CF₄. Bond dissociation energies of UO (7.856(135) eV),

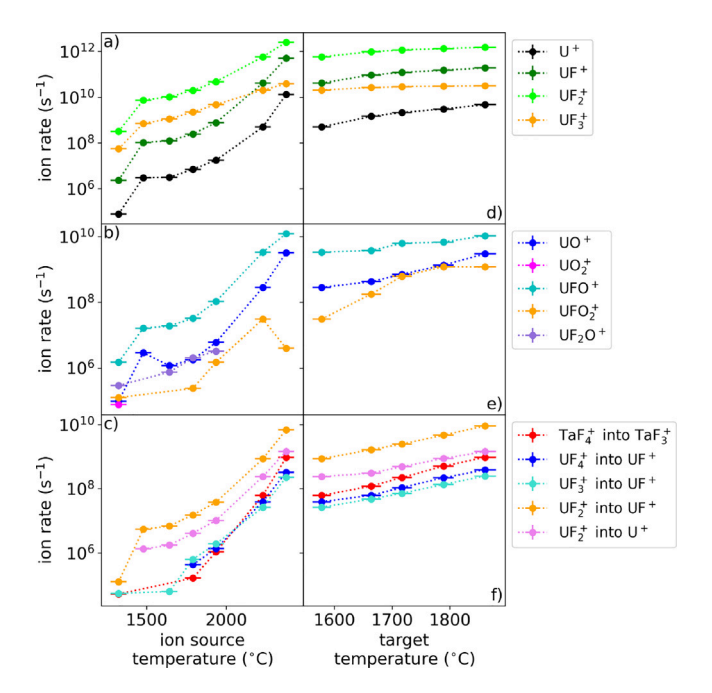


Fig. 4. Rates of ion beams from a tungsten surface ion source recorded on a Faraday Cup after mass separation from the ISOLDE separator magnets shown in logarithmic scale. (a), (b), (c): as a function of ion-source temperature for a target temperature of 1578 °C. (d) (e) (f): rates as a function of target temperature for an ion source temperature of 2230 °C. (c) and (f): rates of fragment ions measured on the apparent mass corresponding to the indicated dissociation of metastable molecular ions.

 UO_2 (7.773(145) eV) [15] suggest that some dissociation of neutral and singly-charged oxides should occur within the FEBIAD ion source.

3.2. Metastable molecular ions

In mass spectrometry, the term 'metastable' is used to describe molecular ions possessing sufficient excess energy to fragment in the field-free region after leaving the ion source [16]. Upon fragmentation, the fragment ions retain a fraction of the kinetic energy of the extracted precursor ion. This causes fragment ions to pass through the mass separator magnetic field with an apparent mass m^* corresponding to [16]

$$m^* = \frac{m_f^2}{m_p} \tag{1}$$

where m_f represents the mass of the fragment ion and m_p represents the mass of the precursor metastable molecular ion. Fragment ions and their precursors were identified from the apparent mass and studied as a function of the target and surface ion source temperatures (Fig. 4). Increasing the ion source temperature significantly increased the fragment ion intensity, suggesting that at high temperatures, the molecules are more likely to have sufficient excess energy to reach the metastable states that fragment after extraction. Fragment molecules are indicated where observed in Fig. 3. Rates of U+, UF+ $_{1,2,3}$ and UF $_{\rm x}$ O $_{\rm y}$ also increase with ion source temperature as surface ionization efficiency increases. This increase could also partially result from increased molecular fragmentation into ionic species occurring in the ion source.

4. In-trap molecular formation

To study in-trap molecular formation, the ISOLTRAP RFQ-cb was employed with a buffer gas (here He at up to $10^{-5}\,\mathrm{mbar}$ measured within 1 m of the injection) to cool and bunch the ions. Mass-separated beams ionized using each of the studied ion sources were sent to the RFQ-cb for cooling and bunching. For studies of beam composition and in-trap molecular formation, a sample of the continuous ion beam was

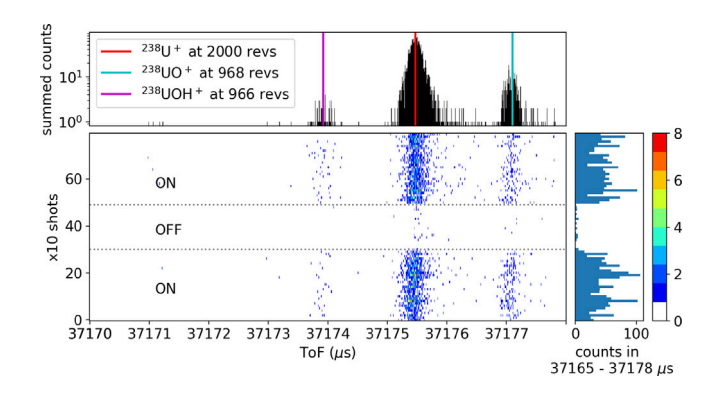


Fig. 5. ToF spectrum of A=238 mass-separated ion beams after cooling and bunching in the ISOLTRAP RFQ-cb, then trapping for 2000 revolutions in the MR-ToF MS as calculated for 238 U. The status of the U resonant laser (on or off) is indicated. Vertical lines shown in the top panel indicate ToFs expected from offline calibrations. See text for further details.

taken into the RFQ-cb. Ions were confined in the RFQ-cb for a trapping time during which interaction occurred between the ions, the buffer gas and residual gas contamination. The ion bunch was then ejected from the RFQ-cb and the arrival times of ions in each shot were measured with respect to the ejection time. Identification was performed with the MR-ToF MS using expected ToF values extracted from a calibration using ^{85,87}Rb⁺, ¹³³Cs⁺ from the ISOLTRAP offline ion source [17], and online ²³⁸U⁺ from ISOLDE. ToF spectra were accumulated over a number of shots as seen in Figs. 5, 6, and 7.

The atomic uranium resonant laser ionization scheme in the ion source affected the count rates of uranium molecules (e.g. UO+ and UOH+ in Fig. 5) observed from the RFQ-cb ion trap. Combined with the mass-separation step of the separator magnets, this indicates that the molecules are formed from ions in the mass-separated U+ beam rather than in the target or ion source. For U and Ta, ratios depend on the trapping time as shown in Figs. 6 and 7. In addition to atomic ions forming molecules, molecular ions mass-separated by ISOLDE (including UF+, UF2+, TaF+, TaF2+) reacted with the residual gas or buffer-gas contaminants to form molecules by pickup of C, O, H and OH (Figs. 7,8) and in some cases (UF+, UF2+) were observed with higher charge states (UF²⁺, UF²⁺). To avoid detector saturation, attenuators were used to reduce the intensity of the ion beam injected into the RFQcb. This reduced absolute rates of in-trap formation and the formation efficiency relative to the ion beam intensity extracted from the ion source. Rates of molecular formation in the ion-trap represent ratios in the regime below space-charge limitations.

Notably, the in-trap UO_x formation showed an identical response to the storage time in the RFQ-cb before and after the addition of a liquid nitrogen cold trap to the buffer gas line, indicating that reaction products enter the ion trap through diffusion into the vacuum chamber rather than buffer gas injection.

5. Conclusions

For previously irradiated or oxidized targets, UO+ and UO $_2^+$ sidebands are on the order of 10^5 ions s $^{-1}$ at target temperatures above 1600 °C. Without further addition of oxygen, the intensity of these contaminants will decrease over time, with the UO $_2^+$ sideband depleting first, followed by the UO+ sideband. At nominal target temperatures (2000 °C) and above, UC+, UC $_2^+$ can similarly reach rates of 10^4 ions s $_2^{-1}$ or more. Fragments formed from the dissociation of metastable U and Ta fluorides arrive as additional non-isobaric contaminants in mass-separated beams. Fragment ions and their precursor ions can be identified using their apparent mass (Eq. (1)) and anticipated for a given mass-to-charge ratio with the rates presented here. We present some representative rates of molecular ions extracted from different ion

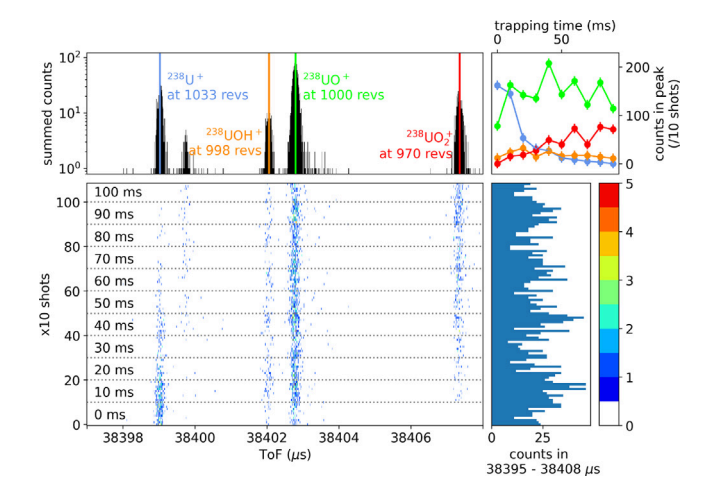


Fig. 6. ToF spectra for various storage times (indicated on the left) of A=238 mass-separated ion beams from the tungsten surface ion source with RILIS for U after cooling and bunching in the ISOLTRAP RFQ-cb, then trapping for 2000 revolutions in the MR-ToF MS as calculated for 238 UO+. Summed counts in each of the identified peaks are shown as a function of trapping time. See text for further details.

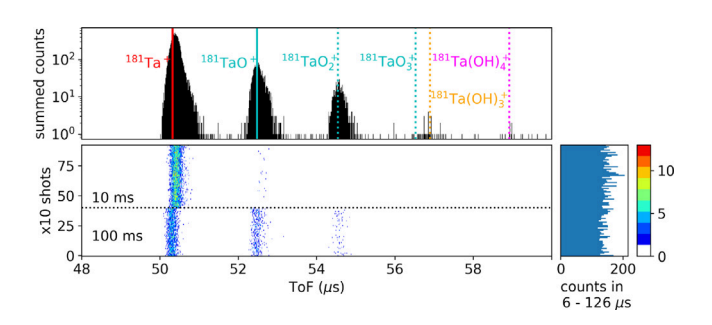


Fig. 7. ToF spectrum of A=181 mass-separated ion beams from the FEBIAD ion source after bunching in the ISOLTRAP RFQ-cb. Cooling time is indicated. Vertical lines in the top panel show ToFs expected from the offline calibration for single-pass operation of the MR-ToF MS.

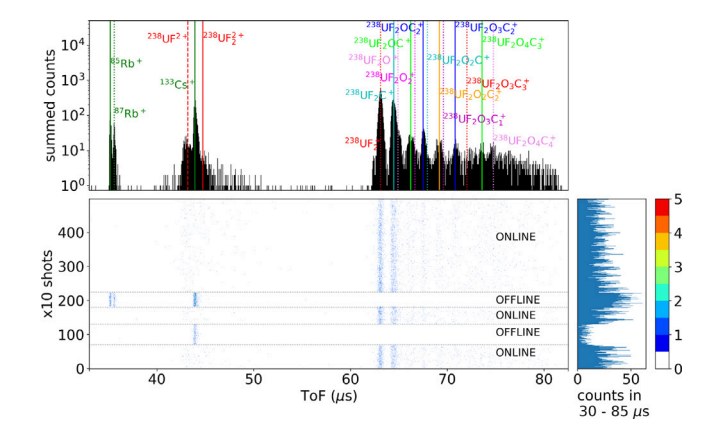


Fig. 8. ToF spectra of A = 276 mass-separated ion beams from a W surface source with CF_4 injection in single-pass operation of the MR-ToF MS with trapping time 200 ms. Horizontal lines show switching between offline reference beam ($^{85,87}Rb^+$, $^{133}Cs^+$). Vertical lines show identified non-isobaric actinide molecules from molecular formation and charge exchange in the ISOLTRAP RFQ-cb.

sources with oxidation, CF_4 , and target temperatures noted in Fig. 4 and Table 1 as well as some representative rates for formation of molecular ions in the RFQ-cb with trapping times noted in Table 2. Rates from the ion source depend very strongly on target and ion source temperature and CF_4 injection rate. Rates from the RFQ-cb depend on trapping time.

Table 1Some observed rates of uranium ion beams from a rhenium surface source and from an electron impact ion source with injected CF₄, recorded on a Faraday cup after mass separation from the ISOLDE mass separator magnet.

| Ion source | Target temperature (°C) | Species | Rate (ions s ⁻¹) |
|-----------------|--------------------------------|---------------------------------------|------------------------------|
| Re surface | 1600 | ²³⁵ U ⁺ | $2.5(1) \times 10^{3}$ |
| previously | 1600 | ²³⁸ U ⁺ | $8.9(6) \times 10^{5}$ |
| irradiated | 1600 | $^{235}U^{16}O^{+}$ | $4.0(6) \times 10^3$ |
| | 1600 | $^{238}U^{16}O^{+}$ | $1.4(2) \times 10^6$ |
| | 1600 | $^{238}U^{18}O^{+}$ | $2.5(9) \times 10^{3}$ |
| | 1600 | $^{235}U^{16}O_{2}^{+}$ | $2.4(1) \times 10^3$ |
| | 1600 | $^{238}U^{16}O_{2}^{+}$ | $7.9(5) \times 10^{5}$ |
| | 1600 | $^{238}U^{16}O^{\tilde{1}8}O^{+}$ | $3.5(5) \times 10^3$ |
| Re surface | 2100 | ²³⁵ U ⁺ | $6.3(1) \times 10^{5}$ |
| previously | 2100 | $^{238}U^{+}$ | $5(1) \times 10^7$ |
| irradiated | 2100 | $^{235}U^{12}C^{+}$ | $7(1) \times 10^3$ |
| | 2100 | $^{235}U^{16}O^{+}$ | $1.24(6) \times 10^4$ |
| | 2100 | $^{238}U^{16}O^{+}$ | $3.3(2) \times 10^6$ |
| | 2100 | $^{238}U^{18}O^{+}$ | $8(1) \times 10^3$ |
| | 2100 | $^{235}U^{12}C_{2}^{+}$ | $4.5(7) \times 10^4$ |
| | 2100 | $^{238}U^{12}C_{2}^{+}$ | $1.3(2) \times 10^7$ |
| | 2100 | $^{238}U^{12}C^{\tilde{1}3}C_{2}^{+}$ | $3(2) \times 10^{5}$ |
| | 2100 | $^{238}U^{16}O_{2}^{+}$ | $7.3(3) \times 10^4$ |
| | 2100 | $^{238}U^{16}O^{\overline{18}}O^{+}$ | $7.4(8) \times 10^{2}$ |
| | 2100 | $^{238}U^{12}C_{3}^{+}$ | $1.3(4) \times 10^4$ |
| FEBIAD | 1818 | $^{238}U^{16}O^{2+}$ | $2.8(5) \times 10^{7}$ |
| with | 1818 | $^{238}U^{16}F^{2+}$ | $6(1) \times 10^{8}$ |
| CF ₄ | 1818 | $^{238}U^{+}$ | $1.5(1) \times 10^{11}$ |
| | 1818 | $^{238}U^{16}O^{+}$ | $3.2(2) \times 10^{11}$ |
| | 1818 | $^{238}U^{19}F^{+}$ | $1.7(1) \times 10^{11}$ |
| | 1818 | $^{238}U^{19}F^{16}O^{+}$ | $1.3(1) \times 10^{10}$ |
| | 1818 | $^{238}U^{19}F_{2}^{+}$ | $1.4(1) \times 10^{11}$ |
| | 1818 | $^{238}U^{19}F^{\tilde{1}6}O_{2}^{+}$ | $3.0(7) \times 10^7$ |
| | 1818 | $^{238}U^{19}F_{2}^{16}O^{+}$ | $3.5(5) \times 10^9$ |
| | 1818 | $^{238}U^{19}F_{3}^{+}$ | $6.8(5) \times 10^{11}$ |
| | 1818 | $^{238}U^{19}F_{4}^{+}$ | $4.9(4) \times 10^{10}$ |

Table 2
Observed rates of ions formed inside the RFQ-cb from initial mass-separated ion beams extracted from a tungsten surface ion source. Counts per seconds of initial beam sampling time were recorded on the ISOLTRAP MagneToF detector after mass separation in the MR-ToF MS. See text for more details.

| Trapping time | Initial ion | Species | Rate |
|---------------|---|--|--------------------------|
| (ms) | beam | | (ions s ⁻¹ of |
| | | | injection time) |
| 5 | ²³⁴ U ⁺ | ²³⁴ U ⁺ | $8.0(8) \times 10^{-2}$ |
| 5 | ²³⁴ U ⁺ | $^{234}UO_{2}H^{+}$ | $9(1) \times 10^{-2}$ |
| 5 | $^{235}U^{+}$ | ²³⁵ U ⁺ | $1.64(5) \times 10^{0}$ |
| 5 | $^{235}U^{+}$ | ²³⁵ UO ₂ ⁺ | $5(1) \times 10^{-2}$ |
| 5 | $^{238}U^{+}$ | ²³⁸ U ⁺ | $4.40(7) \times 10^4$ |
| 5 | $^{238}U^{+}$ | ²³⁸ UO ⁺ | $5.6(2) \times 10^{2}$ |
| 5 | $^{238}U^{+}$ | ²³⁸ UOH ⁺ | $1.5(1) \times 10^{2}$ |
| 5 | ²³⁵ UF ⁺ | ²³⁵ UF ⁺ | $1.39(3) \times 10^4$ |
| 5 | ²³⁵ UF ⁺ | ²³⁵ UFO ⁺ | $3.6(3) \times 10^{2}$ |
| 5 | ²³⁵ UF ⁺ | ²³⁵ UFOH ⁺ | $7(1) \times 10^{1}$ |
| 100 | ²³⁵ UF ⁺ | ²³⁵ UFO ⁺ | $1.16(6) \times 10^4$ |
| 100 | ²³⁵ UF ⁺ | ²³⁵ UFOH ⁺ | $5.2(9) \times 10^{2}$ |
| 100 | ²³⁸ UF ⁺ | ²³⁸ UF ⁺ | $1.39(8) \times 10^{5}$ |
| 100 | ²³⁸ UF ₂ ⁺ | ²³⁸ UF ₂ ⁺ | $1.69(3) \times 10^4$ |
| 100 | ²³⁸ UF ₂ ⁺ | ²³⁸ UF ₂ O ⁺ | $7(1) \times 10^{1}$ |
| 100 | ²³⁸ UF ₂ ⁺ | ²³⁸ UFO ₂ H ⁺ | $1.6(6) \times 10^{1}$ |
| 200 | ²³⁸ UF ₂ ⁺ | ²³⁸ UF ₂ ⁺ | $1.17(2) \times 10^4$ |
| 200 | ²³⁸ UF ₂ ⁺ | ²³⁸ UF ₂ O ⁺ | $3.4(3) \times 10^{2}$ |
| 200 | $^{238}UF_{2}^{+}$ | $^{238}UFO_{2}H^{+}$ | $9.2(1.4) \times 10^{1}$ |
| 200 | ²³⁸ UF ₂ ⁺ | $^{238}UF^{2+}$ | $8.2(9) \times 10^{1}$ |
| 200 | ²³⁸ UF ₂ ⁺ | ²³⁸ UF ₂ ²⁺ | $2.9(5) \times 10^{1}$ |

Production of fluoride molecular ions from the ion source is achieved by adding CF_4 . Since many actinide fluorides are stable at temperatures above 1000 °C, in-source formation is a promising approach that can use parameters including target and ion source temperatures and fluorine partial pressure to control formation rates.

To form molecules that may not be stable at high temperatures, molecular formation in the RFQ ion trap is presented as a possible approach. Formation of oxides, carbides, and hydroxides from the mass-separated atomic and molecular ion beams occurs in the ISOLTRAP RFQ-cb in the presence of residual gases. Trapping time is shown to be a parameter influencing the formation of molecules in the ion trap. The molecular formation reported here in the ISOLTRAP RFQ-cb may have implications for other RFQ-cb ion traps used in beam preparation (e.g. the ISOLDE cooler ISCOOL [2]) which require further investigations.

These studies combined characterize the composition of beams heavier than the target material and provide information on the process of creating molecular actinide beams in targets and in ion traps.

Declaration of competing interest

The authors declare that they have no known competing financial interests or personal relationships that could have appeared to influence the work reported in this paper.

Acknowledgments

The authors gratefully acknowledge support from the ISOLDE operations team, the ISOLDE targets and ion sources team, and Simone Gilardoni. This project has received funding from the European Union's Horizon 2020 Research and Innovation Program (grant No. 861198 project 'LISA' MSC ITN). The authors acknowledge support from the German Federal Ministry of Education and Research (BMBF) for ISOLTRAP (grant No. 05P18HGCIA and 05P21HGCI1). L.N. acknowledges support from the Wolfgang Gentner Program (grant No. 13E18CHA).

References

- [1] G. Arrowsmith-Kron, M. Athanasakis-Kaklamanakis, M. Au, J. Ballof, R. Berger, A. Borschevsky, A.A. Breier, F. Buchinger, D. Budker, L. Caldwell, C. Charles, N. Dattani, R.P. de Groote, D. DeMille, T. Dickel, J. Dobaczewski, C.E. Düllmann, E. Eliav, J. Engel, M. Fan, V. Flambaum, K.T. Flanagan, A. Gaiser, R.G. Ruiz, K. Gaul, T.F. Giesen, J. Ginges, A. Gottberg, G. Gwinner, R. Heinke, S. Hoekstra, J.D. Holt, N.R. Hutzler, A. Jayich, J. Karthein, K.G. Leach, K. Madison, S. Malbrunot-Ettenauer, T. Miyagi, I.D. Moore, S. Moroch, P. Navrátil, W. Nazarewicz, G. Neyens, E. Norrgard, N. Nusgart, L.F. Pašteka, A.N. Petrov, W. Plass, R.A. Ready, M.P. Reiter, M. Reponen, S. Rothe, M. Safronova, C. Scheidenberger, A. Shindler, J.T. Singh, L.V. Skripnikov, A.V. Titov, S.-M. Udrescu, S.G. Wilkins, X. Yang, Opportunities for fundamental physics research with radioactive molecules, 2023, http://dx.doi.org/10.48550/ARXIV.2302.02165, arXiv, URL https://arxiv.org/abs/2302.02165.
- [2] R. Catherall, W. Andreazza, M. Breitenfeldt, A. Dorsival, G.J. Focker, T.P. Gharsa, T.J. Giles, J.L. Grenard, F. Locci, P. Martins, S. Marzari, J. Schipper, A. Shornikov, T. Stora, The ISOLDE facility, J. Phys. G: Nucl. Part. Phys. 44 (9) (2017) http://dx.doi.org/10.1088/1361-6471/aa7eba.
- [3] J. Ballof, C. Seiffert, B. Crepieux, C.E. Düllmann, M. Delonca, M. Gai, A. Gottberg, T. Kröll, R. Lica, M. Madurga Flores, Y. Martinez Palenzuela, T.M. Mendonca, M. Owen, J.P. Ramos, S. Rothe, T. Stora, O. Tengblad, F. Wienholtz, Radioactive boron beams produced by isotope online mass separation at CERN-ISOLDE, Eur. Phys. J. A 55 (5) (2019) http://dx.doi.org/10.1140/epja/i2019-12719-1.

- [4] U. Köster, O. Arndt, E. Bouquerel, V.N. Fedoseyev, H. Frånberg, A. Joinet, C. Jost, I.S. Kerkines, R. Kirchner, Progress in ISOL target–ion source systems, Nucl. Instrum. Methods Phys. Res. B 266 (19–20) (2008) 4229–4239, http://dx.doi.org/10.1016/J.NIMB.2008.05.152.
- [5] U. Köster, P. Carbonez, A. Dorsival, J. Dvorak, R. Eichler, S. Fernandes, H. Frånberg, J. Neuhausen, Z. Novackova, R. Wilfinger, A. Yakushev, (IM-)possible ISOL beams, Eur. Phys. J.: Special Topics 150 (2007) 285–291, http://dx.doi.org/10.1140/epjst/e2007-00326-1.
- [6] R. Eder, H. Grawe, E. Hagebø, P. Hoff, E. Kugler, H.L. Ravn, K. Steffensen, The production yields of radioactive ion-beams from fluorinated targets at the ISOLDE on-line mass separator, Nuclear Inst. Methods Phys. Res. B 62 (4) (1992) 535–540, http://dx.doi.org/10.1016/0168-583X(92)95387-7.
- [7] L.V. Skripnikov, N.S. Mosyagin, A.V. Titov, V.V. Flambaum, Actinide and lanthanide molecules to search for strong CP-violation, Phys. Chem. Chem. Phys. 22 (33) (2020) 18374–18380, http://dx.doi.org/10.1039/d0cp01989e, arXiv: 2003.10885.
- [8] M.S. Safronova, D. Budker, D. Demille, D.F. Kimball, A. Derevianko, C.W. Clark, Search for new physics with atoms and molecules, Rev. Modern Phys. 90 (2) (2018) http://dx.doi.org/10.1103/RevModPhys.90.025008, arXiv:1710.01833.
- [9] T.A. Isaev, S. Hoekstra, R. Berger, Laser-cooled RaF as a promising candidate to measure molecular parity violation, Phys. Rev. A 82 (2010) 052521, http://dx.doi.org/10.1103/PhysRevA.82.052521, URL https://link.aps.org/doi/10.1103/PhysRevA.82.052521.
- [10] L. Penescu, R. Catherall, J. Lettry, T. Stora, Development of high efficiency Versatile Arc Discharge Ion Source at CERN ISOLDE, Rev. Sci. Instrum. 81 (2) (2010) 1–5, http://dx.doi.org/10.1063/1.3271245.
- [11] V. Fedosseev, K. Chrysalidis, T.D. Goodacre, B. Marsh, S. Rothe, C. Seiffert, K. Wendt, Ion beam production and study of radioactive isotopes with the laser ion source at ISOLDE, J. Phys. G: Nucl. Part. Phys. 44 (8) (2017) http: //dx.doi.org/10.1088/1361-6471/aa78e0.
- [12] F. Herfurth, J. Dilling, A. Kellerbauer, G. Bollen, S. Henry, H.-J. Kluge, E. Lamour, D. Lunney, R. Moore, C. Scheidenberger, S. Schwarz, G. Sikler, J. Szerypo, A linear radiofrequency ion trap for accumulation, bunching, and emittance improvement of radioactive ion beams, Nucl. Instrum. Methods Phys. Res. A 469 (2) (2001) 254–275, http://dx.doi.org/10.1016/S0168-9002(01)00168-1, URL https://www.sciencedirect.com/science/article/pii/S0168900201001681.
- [13] R.N. Wolf, F. Wienholtz, D. Atanasov, D. Beck, K. Blaum, C. Borgmann, F. Herfurth, M. Kowalska, S. Kreim, Y.A. Litvinov, D. Lunney, V. Manea, D. Neidherr, M. Rosenbusch, L. Schweikhard, J. Stanja, K. Zuber, ISOLTRAP's multi-reflection time-of-flight mass separator/spectrometer, Int. J. Mass Spectrom. 349–350 (1) (2013) 123–133, http://dx.doi.org/10.1016/j.ijms.2013.03.020.
- [14] M.R. Savina, B.H. Isselhardt, R. Trappitsch, Simultaneous isotopic analysis of U, Pu, and Am in spent nuclear fuel by resonance ionization mass spectrometry, Anal. Chem. 93 (27) (2021) 9505–9512, http://dx.doi.org/10.1021/acs. analchem.1c01360.
- [15] L.R. Morss, N.. Edelstein, J. Fuger, J.J. Katz, Chemistry of Actinide and Transactinide Elements, fourth ed., Springer, 2010.
- [16] R.A.W. Johnstone, M.E. Rose, Mass Spectrometry for Chemists and Biochemists, Cambridge University Press, 2012, pp. 232–288, http://dx.doi.org/10.1017/ cbo9781139166522.009.
- [17] F. Wienholtz, D. Beck, K. Blaum, C. Borgmann, M. Breitenfeldt, R.B. Cakirli, S. George, F. Herfurth, J.D. Holt, M. Kowalska, S. Kreim, D. Lunney, V. Manea, J. Menéndez, D. Neidherr, M. Rosenbusch, L. Schweikhard, A. Schwenk, J. Simonis, J. Stanja, R.N. Wolf, K. Zuber, Masses of exotic calcium isotopes pin down nuclear forces, Nature 498 (7454) (2013) 346–349, http://dx.doi.org/10.1038/nature12226.